

POLYCARBONATE URETHANE-HYDROXYPROPYL CELLULOSE MEMBRANES WITH ZINC OXIDE NANOPARTICLES

STELIAN VLAD,* LUIZA M. GRADINARU,*
CONSTANTIN CIOBANU,* DOINA MACOCINSCHI,* DANIELA FILIP,*
IULIANA SPIRIDON* and ROBERT V. GRADINARU**

*“Petru Poni” Institute of Macromolecular Chemistry, 41A, Grigore Ghica Voda Alley,
700487 Iasi, Romania

**Department of Chemistry, “Al. I. Cuza” University, 700506, Iasi, Romania

✉ Corresponding author: S. Vlad, vladus@icmpp.ro

Received January 2015

Polycarbonate urethane-hydroxypropyl cellulose (PCU-HPC) membranes were synthesized and the impact of adding progressive amounts of zinc oxide nanoparticles (ZnONPs) on the morphological, thermal, mechanical, wetting and antibacterial properties of the membranes was investigated. Materials characterization was performed by Fourier transform infrared spectroscopy (FTIR), environmental scanning electron microscopy (ESEM), thermogravimetric analysis (TGA), dynamic vapour sorption (DVS), contact angle (CA) and mechanical testing. Results showed that Young's modulus and tensile strength increased, while elongation at break decreased. All membranes presented good antibacterial activity against *Escherichia coli*.

Keywords: polyurethane, cellulose derivative, nanoparticles, antibacterial activity

INTRODUCTION

Polyurethanes (PUs) are a particularly interesting class of materials, and have been thus the focus of many researches in recent years.¹⁻⁵ The outstanding qualities of these materials make them such a redoubtable candidate for various industries and for medical applications.⁶⁻¹⁰ Therefore, it is easy to understand why they have found numerous applications in coating, textile, oil, foods, car industry, etc.¹¹⁻¹⁵ In addition, many types of PUs, including polycarbonate urethane (PCU), have good biocompatibility with the human body and are used for various implants such as heart valves, patches, blood vessels, drug delivery etc.¹⁶⁻²⁰ The application of PCU has been the object of several studies.²¹⁻²³ Zinc oxide nanoparticles (ZnONPs) are useful as antibacterial and antifungal agents when incorporated into materials.^{24,25} The enhanced surface area of zinc oxide allows an increased interaction with bacteria.²⁶ Thus, it is possible to use small quantities of zinc oxide to achieve the same or improved performance. Cellulose derivatives are

widely used obtain polymer mixtures, aiming their use in the biomedical field.^{27,28} Their effect is to enhance the biodegradability of the new polymers.²⁹ HPC is one of the most often used derivatives in combination with urethane polymers.^{30,31} The influence of HPC in a matrix of polyurethane materials has been investigated with the objective to improve the biocompatibility and biodegradability of devices for biomedical applications.^{17,32} Also, such materials have been studied for the controlled release of drugs and biologically active principles.¹⁹ The introduction of Ag, Zn, etc nanoparticles into a polyurethane matrix leads to an increase in the antibacterial and/or antifungal activity of these materials.^{24,25}

The aim of this study was to investigate the influence of progressive amounts of ZnONPs on the properties of new membranes comprising PCU and HPC. The structure and morphology of these membranes were analyzed by FTIR and ESEM. Thermogravimetric analysis, contact angle measurements, dynamic vapour sorption

and mechanical testing were also carried out to characterize all obtained materials. The antibacterial activity against *Escherichia coli* (*E. coli*) was investigated as well.

EXPERIMENTAL

Materials

Poly(hexamethylene carbonate) diol (average Mn 2000, Aldrich); 1,6-hexamethylene diisocyanate (Fluka); dimethylolpropionic acid (Fluka); 1,4-butane diol (Sigma Aldrich); zinc oxide nanoparticles powder, (size < 100 nm – Aldrich); hydroxypropyl cellulose (powder, average Mn ~10000, Sigma Aldrich); dibutyltin dilaurat (DBTL-Fluka); dimethylformamide (DMF- Fluka) were used in our study. Commercial DMF was dried over anhydrous K₂CO₃, and then it was distilled from calcium hydride (CaH₂) and kept over 4 Å molecular sieves. Polyol and chain extender were checked for moisture, and if necessary, it was lowered below 0.3%. The other chemicals were used as received without further purification. For the biological test, Luria Bertani (LB) medium (10 g Bacto Tryptone, 5 g yeast extract, 5 g NaCl; pH = 7.0) and *E. coli* cells (strain DH5α, T7 Express Sampler, New England, BioLabs) were used.

Synthesis of urethane prepolymer based on PHC and HDI

PHC was dried in vacuum (1 mmHg) at 85 °C, under stirring for 3 h. Then, at atmospheric pressure, a necessary amount of HDI and DMF were added. 2-3 drops of DBTL were used as catalyst. This mixture

was kept for 4 h at 80 °C under stirring (80-100 rpm), to form a urethane prepolymer solution. The molar ratio for PHC:HDI was of 1:2 (Scheme 1).

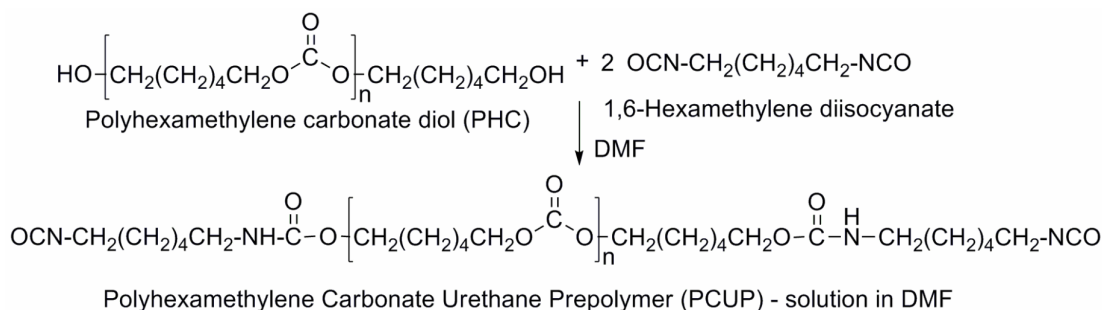
Synthesis of urethane prepolymer based on DMPA and HDI

In step II, DMPA dissolved in DMF and the necessary amount of HDI, in a molar ratio of DMPA:HDI 1:2, was reacted to form a urethane prepolymer. The reaction was carried out at atmospheric pressure and 60 °C temperature, under stirring for 8 h, when dimethylpropionic acid urethane prepolymer (DMPAUP) was obtained (Scheme 2). In this stage, 2-3 drops of DBTL were used as catalyst.

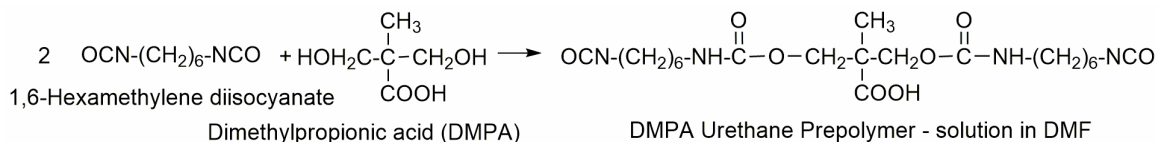
Synthesis of PCUP with DMPA

In step III, the PCUP and DMPAUP solution were mixed together, under stirring at 80 °C, for 1 h. By the reaction of OH groups from the chain extender (BD) with NCO end-groups, a new polyurethane solution (PCU) was obtained (Scheme 3).

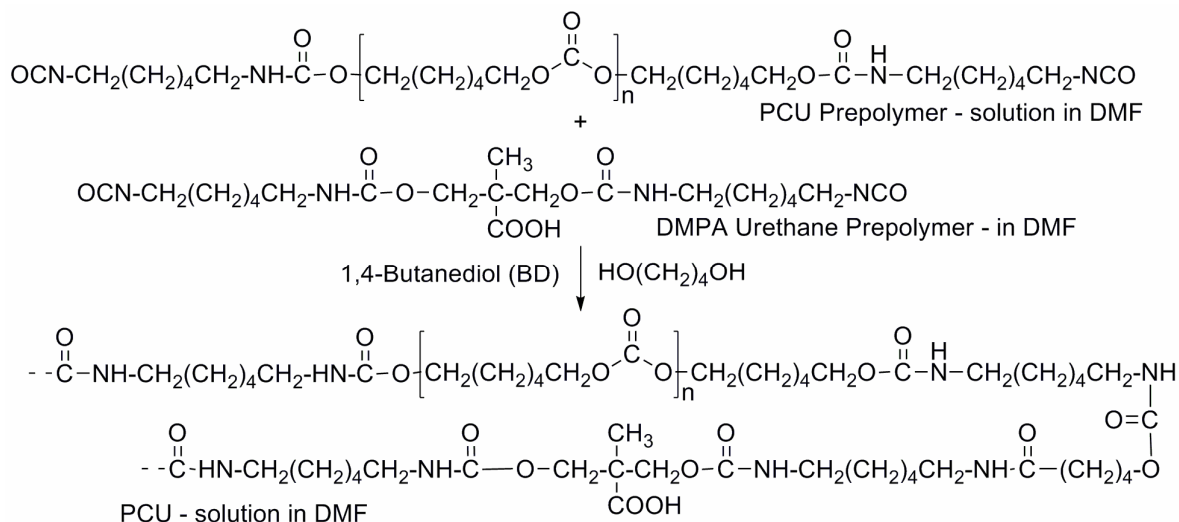
Finally, a PCU 25% w/w solution in DMF, with hard-segment content (HDI and BD) of 19% w/w was obtained. 4 g HPC was mixed with 6 g DMF and sonicated for 10 minutes. 40 g of PCU solution was mixed with the solution of HPC. This PCU-HPC solution was divided into 4 portions. Separately, a quantity of 2.5 g ZnONPs powder < 100 nm was mixed with 7.5 g DMF and sonicated for 10 minutes. Portions of this suspension were used for preparing PCU-HPC samples (e.g.: 1 g of suspension containing 0.25 g of ZnONPs).



Scheme 1: Synthesis of poly(hexamethylene carbonate) urethane prepolymer (PCUP)



Scheme 2: Synthesis of urethane prepolymer based on DMPA and HDI (DMPAUP)



Scheme 3: Synthesis of poly(hexamethylene carbonate) urethane

Sample preparation

In 20 ml vials, 12.5 g of PCU-HPC solution and different quantities (0.25, 0.5, 0.75 and 1.0 g respectively) of ZnONPs suspension were added. The vials were stirred for 72 h at 50 °C. Afterwards, the mixture was poured on a glass plate to form a film, which was then precipitated in warm water (at 45 °C). The resulting samples, noted as PCU-HPC1 (comprising 0.25 g ZnONPs), PCU-HPC2 (0.5 g ZnONPs), PCU-HPC3 (0.75 g ZnONPs) and PCU-HPC4 (1 g ZnONPs), were characterized and assessed with respect to the influence of ZnONPs on their morphological properties, thermal behaviour, wetting properties, mechanical performance and antibacterial activity.

Methods

Infrared spectroscopy: ATR-FTIR technique was used to examine changes in the molecular structures of the samples before and after mixing with ZnONPs. The spectra were recorded on a Bruker Vertex 70 FT-IR instrument, equipped with a Golden Gate single reflection ATR accessory, in the spectrum range 600-4000 cm^{-1} and a spectral resolution of 2 cm^{-1} at ambient temperature.

Thermogravimetric analysis: TG analysis was performed using a Netzsch STA 449 F1 Jupiter system under nitrogen atmosphere. The measurements were performed heating the samples (≈ 5 mg) placed in Al_2O_3 crucibles hermetically closed with lids, at a rate of 10 $^\circ\text{C}\cdot\text{min}^{-1}$, from room temperature up to 600 $^\circ\text{C}$, using nitrogen as purging gas at a flow rate of 50 $\text{mL}\cdot\text{min}^{-1}$.

Surface characterization: Surface morphology was examined using a SEM/ESEM FEI Quanta 200 microscope equipped with EDAX Si (Li) X-ray detector and Gatan Alto Cyro stage, operating at 20 kV.

Samples were mounted on graphite supports and observed under different degrees of magnification. Images of cross-sections were taken from the most relevant aspects.

Contact angle: Contact angles were measured using the sessile-drop technique at room temperature, and a KSV CAM 101 goniometer, equipped with a special optical system and a CCD camera connected to a computer to capture and analyze the contact angle (five measurements for each surface). A drop of liquid (≈ 1 μl) was placed, with a Hamilton syringe, on a specially prepared plate of substratum and the image was sent *via* the CCD camera to the computer for analysis. The measurements were carried out at 25 $^\circ\text{C}$ and 65% relative humidity.

Dynamic vapour sorption: DVS was used for determination of the sorption/desorption isotherms. For this, a fully automated gravimetric analyzer IGA_{sorp} supplied by Hiden Analytical, Warrington (UK) was used. An ultra-sensitive microbalance (0.1 μg resolution for 100 mg range and a 200 mg capacity) was employed. By mixing wet and dry gas (N_2) streams, the level of humidity is controlled to the desired relative humidity (RH) set-point (the measurement range of RH is between 1% and 95% RH with an accuracy of $\pm 1\%$ (0%-90% RH) and $\pm 2\%$ (90%-95% RH) and the measurement range of temperature is between 5 $^\circ\text{C}$ and 80 $^\circ\text{C}$ with an accuracy of ± 0.05 $^\circ\text{C}$). The sample container is a gas-permeable micromesh stainless pan for solids. The samples are dried at 25 $^\circ\text{C}$ under flowing nitrogen until the weight of each sample is in equilibrium at RH < 1% and the resulting value is considered the dry mass. Following drying, the absorption curve is determined. Once the maximum level for RH has been reached, desorption steps can be obtained.

Tensile characterization: Stress-strain measurements were performed on a TIRA test 2161 apparatus, Maschinenbau GmbH Ravenstein, Germany, on dumbbell-shaped cut samples with dimensions of 50x8.5x4 mm. Measurements were run at 25 °C, humidity of 60% and an extension rate of 20 mm/min. All reported results represent the averages of three measurements.

Antibacterial activity: The antibacterial activity of the materials was estimated based on a modified minimum inhibitory concentration method.³³ All the experiments were performed in Luria Bertani (LB) medium (10 g Bacto Tryptone, 5 g yeast extract and 5 g NaCl were dissolved in 0.8 L bidistilled water; pH was adjusted with 1 mL NaOH 1 M to 7.0 and the final volume to 1 L). The medium was further poured in flasks and autoclaved for 30 min at 120 °C. A preculture was obtained by growing the *E. coli* (strain DH5a, T7 Express Sampler, New England, BioLabs) for 20 h at 28 °C with continuous stirring (50 rpm), in a 200 mL flask containing 40 mL sterile medium. Afterwards, sterile 100 mL Erlenmeyer flasks, each containing 20 mL of LB medium, were inoculated using 1 mL preculture (optical density OD 1.15) and grown at 37 °C and 100 rpm. The cell density was monitored at 5 and 20 h respectively, by reading sample absorbance (OD) as against LB sterile medium at 580 nm using a Libra UV/Vis Spectrophotometer (Biochrom, Cambridge, UK). Before using, the samples were sterilized by autoclaving at 120 °C. All results represent average of three measurements.

RESULTS AND DISCUSSION

FTIR characterization

The formation of urethane linkage is confirmed by the disappearance of NCO stretching band at 2272 cm⁻¹ (Figure 1) from the FTIR spectra of all membranes. The main

characteristic absorption peaks of the samples' spectra are summarized in Table 1.

The samples comprising ZnONPs were characterized by an increase in peak intensity from 1681 cm⁻¹. Also, a new peak between 1626-1623 cm⁻¹ occurred, probably due to the reaction between acidic groups of DMPA from PCU, HPC and ZnONPs. HPC acts as a binder between PCU and nanoparticles, causing an increase in peak intensity.

Thermo-gravimetric analysis

Kinetic parameters, such as activation energy (Ea) and reaction order (n) were obtained using the Coats-Redfern method and the Versatile 1.0 software.³⁴ The decomposition upon heating was observed in three stages (Figure 2) and the reaction order was around 2 (Table 2). All samples presented the first stage of decomposition over 280 °C, which demonstrates a good thermal resistance. The addition of different percentages of ZnONPs in PCU-HPC resulted in an increase of the residue 'amount. Thus, large percentages of residue indicate that ZnONPs reacts with acid groups of DMPA from PCU, which is also proved by decrease of polar component of surface free energy (see Table 3).

Wetting properties

The wetting characteristics of the studied materials are discussed with respect to the contact angle, work of adhesion, surface free energy and diffusion coefficients of PCU and PCU-HPC membranes comprising ZnONPs (Table 3).

Table 1
Main characteristic bands present in the FTIR spectra of the polymer samples

Wavenumbers (cm ⁻¹)	Bonds	Vibrational modes
3317	O-H (hydroxyl); N-H	Stretching
2917, 2850	C-H (methylene)	Asymmetrical and symmetrical bending
1740	C=O (carbonyl)	Stretching
1681, 1536	CO-N (amide I and II)	Stretching
1461, 1402	C-H (methylene)	Asymmetrical and symmetrical bending
1246	R-NH-COO- (amide III)	Stretching
1140, 1070	CO-O-C (ester)	Stretching
970, 1040	O-C=O	Stretching
791	CO-O-C (ester)	out-of-plane bending

Table 2
Overall kinetic parameters of materials decomposition

Sample	n, I/II/III	Ea, KJ/mol I/II/III	Weight loss, %			Residue, %
			Stage I 200-300 °C	Stage II 300-400 °C	Stage III 400-500 °C	
PCU	1.7/1.9/2.1	178/188/229	31.1	46.3	19.8	2.8
PCU-HPC2	1.8/1.9/1.8	211/214/182	26.1	38.7	11.0	24.2
PCU-HPC4	1.7/1.8/1.7	187/178/149	21.4	31.1	10.2	37.3

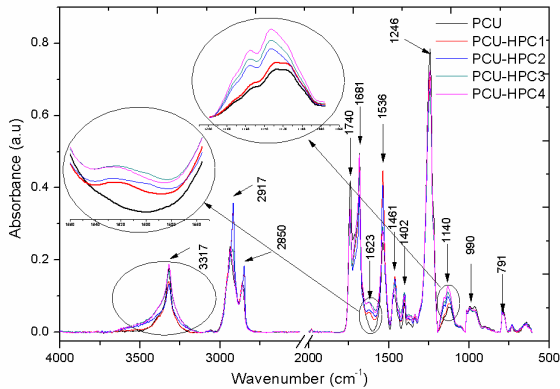


Figure 1: ATR-FTIR spectra of PCU and PCU-HPC with ZnONPs

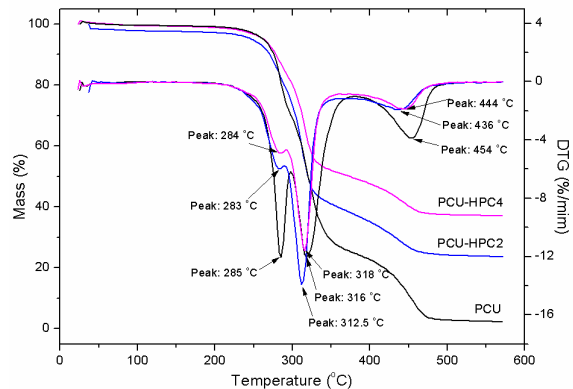


Figure 2: TG and DTG curves of PCU, PCU-HPC2 and PCU-HPC4

Table 3
Surface properties of the studied materials

Sample	CA, deg	WA, mN/m	SFE (γ_{SV}), mN/m	Polar component (γ_{SV}^p), mN/m	Dispersive component (γ_{SV}^d), mN/m	SFE (γ_{SL}), mN/m
PCU	93.91	67.84	17.77	6.550	11.220	22.74
PCU-HPC1	111.25	46.41	12.42	1.100	11.320	38.81
PCU-HPC2	111.72	45.86	22.29	0.020	22.270	49.23
PCU-HPC3	113.65	43.59	17.56	0.100	17.460	46.77
PCU-HPC4	116.07	40.81	18.34	0.003	18.336	50.36

CA – contact angle; WA – work of adhesion; SFE – surface free energy

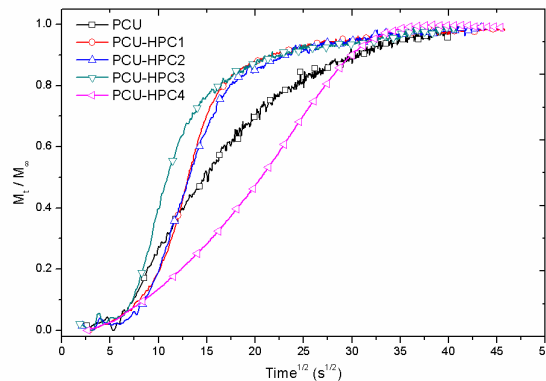


Figure 3: Normalized mass change as a function of square root of time for the studied materials

The contact angles of the materials increase in the order: PCU < PCU-HPC1 < PCU-HPC2 < PCU-HPC3 < PCU-HPC4, proving that the increment in the amount of ZnONPs increased hydrophobicity. The surface free energy of the samples was particularly influenced by the polar component, which is due to the polar functional groups. Thereby, a lower amount of polar component corresponds to a pronounced hydrophobic character, respectively to low wettability, which affects the growth of *E. coli*.

Based on the experimental data of the sorption-desorption isotherms, Crank³⁵ and then Balik³⁶ developed various methods for determining the diffusion coefficients based on Fick's second equation.

As indicated in a previous study,³⁷ the diffusion coefficient (*D*) can be obtained from a plot giving the ratio of the swollen polymer mass at time *t* and *t*=∞ (corresponding to sorption equilibrium), the initial slope of a plot of *M_t/M_∞* as a function of the square root of time *t*^{1/2} or the limiting slope of a plot of *ln(1 - M_t/M_∞)* vs. *t* (Figure 3). At sufficiently *short* times, Eq. 1 becomes determinant:

$$\frac{M_t}{M_\infty} = \frac{4}{l} \cdot \sqrt{\frac{D_1 \cdot t}{\pi}} \quad (1)$$

so: $(M_t/M_\infty)^2 = 16 \cdot D_1 \cdot t / \pi \cdot l^2 = K_1 \cdot t$, where: $K_1 = 16 \cdot D_1 / \pi \cdot l^2$, result: $D_1 = K_1 \pi l^2 / 16$.

At sufficiently *long* times, Eq. 2 becomes determinant:

$$\frac{M_t}{M_\infty} = 1 - \frac{8}{\pi^2} \cdot e^{-\frac{D_2 \pi^2 t}{l^2}} \quad (2)$$

so: $\ln(1 - M_t/M_\infty) = \ln 8 / \pi^2 - D_2 \cdot \pi^2 \cdot t / l^2 = K_2 \cdot t$, where: $K_2 = -D_2 \cdot \pi^2 / l^2$, result: $D_2 = -K_2 l^2 / \pi^2$.

Data from Table 4 show that for short periods of time (*M_t/M_∞* < 0.5), the diffusion coefficient increases with an increase in the ZnONPs content, but it is lower with an order of magnitude than that of the sample without zinc oxide. For long periods of time (*M_t/M_∞* > 0.5), the diffusion coefficients have similar values, favouring a balance, which is less influenced by the content of ZnONPs added into the samples.

Mechanical tests

The stress-strain curves of the samples are shown in Figure 4. Mechanical properties are presented in Table 5. The tensile strength of the polyurethane samples is affected by factors such as the content of soft and hard segments in the polymer structure, their cohesion energy, the packing degree of macromolecules, phase separation, the cross-linking degree of polymer samples, etc.³⁸ It is evident that the mechanical characteristics are influenced by the percentage of ZnONPs in the sample.

Table 4
Diffusion coefficients determined from the experimental data of the studied polymers

Sample	<i>K₁</i> [*] ,	<i>K₂</i> [*] ,	<i>l</i> (cm)	<i>D₁</i> = <i>K₁</i> π <i>l</i> ² /16 (cm ² /s)	<i>D₂</i> =- <i>K₂</i> <i>l</i> ² /π ² (cm ² /s)
	<i>M_t/M_∞</i> <0.5	<i>M_t/M_∞</i> >0.5			
PCU	2.90·10 ⁻²	-2.02·10 ⁻³	9·10 ⁻²	4.61·10 ⁻⁵	1.66·10 ⁻⁶
PCU-HPC1	1.54·10 ⁻³	-2.38·10 ⁻³	9·10 ⁻²	2.45·10 ⁻⁶	1.95·10 ⁻⁶
PCU-HPC2	1.78·10 ⁻³	-2.23·10 ⁻³	9·10 ⁻²	2.83·10 ⁻⁶	1.83·10 ⁻⁶
PCU-HPC3	2.70·10 ⁻³	-1.77·10 ⁻³	9·10 ⁻²	4.29·10 ⁻⁶	1.45·10 ⁻⁶
PCU-HPC4	6.17·10 ⁻⁴	-4.43·10 ⁻²	9·10 ⁻²	9.81·10 ⁻⁷	3.64·10 ⁻⁶

* *K₁* is the slope of linear regression between (t-t_R) and (M_t/M_∞)² for (t-t_R) ≥ 0 and (M_t/M_∞)² < 0.2; t_R – time correlation for M_t/M_∞=0; *K₂* is the slope of linear regression between t and ln(1- M_t/M_∞) for -1.2 > ln < -3.0

Table 5
Main physico-mechanical characteristics of the studied materials

Sample	Young's modulus, MPa	Tensile strength, MPa	Elongation at break, %	Hardness, °ShA	Toughness, KJ·m ⁻³
PCU	168.39	7.70	89.20	55	59.72
PCU-HPC1	265.89	9.65	89.45	58	49.82
PCU-HPC2	307.84	9.52	29.68	62	26.96
PCU-HPC3	361.31	11.15	14.30	65	14.15
PCU-HPC4	502.82	13.64	11.24	70	12.34

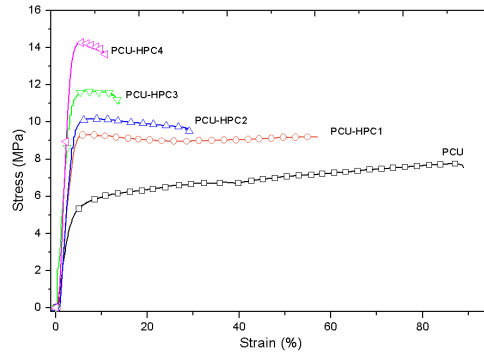


Figure 4: Stress-strain curve of the studied membranes

Young's modulus and tensile strength of the materials are significantly improved by the addition of ZnONPs, to the detriment of elongation. In addition, hardness increases with the amount of ZnONPs. Tensile toughness represents the quantity of energy per volume that can be absorbed by the material before failure. It is estimated as the area for each stress-strain curve, and can be indirectly correlated with the energy released by an elastic material when the force that acted on it is removed, like in a harvesting energy system. PCU-HPC with lower amounts of ZnONPs (PCU-HPC1 and PCU-HPC2) absorbs more energy per volume before failure, as compared to the samples comprising higher contents of ZnONPs.

Morphological aspects

Figure 5 presents SEM images of the porous PCU and PCU-HPC membranes. Pore sizes up to 47 μm (PCU), 105 μm (PCU-HPC1), 115 μm (PCU-HPC2), 120 μm (PCU-HPC3) and 132 μm (PCU-HPC4) were measured using Image J 1.47v

software (<http://imagej.nih.gov/ij>). This kind of porosity can be considered adequate for good antibacterial activity. From the SEM images, it is also observed that the pore size increases with the content of ZnONPs.

Antibacterial activity

PCU-HPC membranes were screened for antibacterial activity. A simple spectroscopic analysis reveals that the optical density (OD) of the cell culture within the flask containing the PCU-HPC membranes embedded with ZnONPs presented lower values, as compared to the control sample (PCU).

Bacterial cell viability was quantified after 5 and 20 h and is illustrated in Figure 6. The *E. coli* viability decreases with an increase in the ZnONPs embedded in PCU-HPC, revealing a good antibacterial activity of these materials. An increase of pore diameter of the membranes from 47 to 105 μm will generate a larger active surface (up to five times) and volume (up to ten times), respectively.

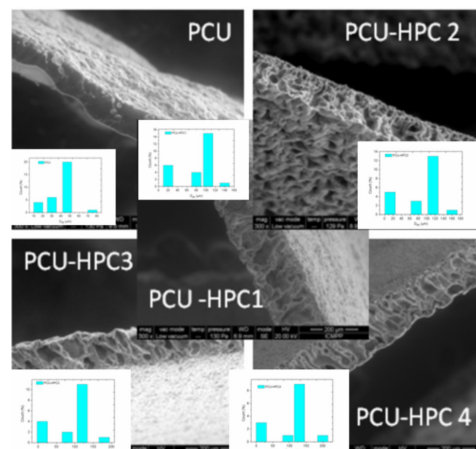


Figure 5: SEM images of the cross section of PCU and PCU-HPC membrane with ZnONPs

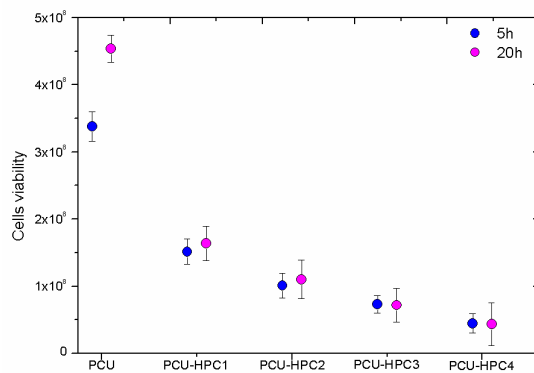


Figure 6: Cell viability of the studied materials after 5 and 20 h, respectively

However, *E. coli* could easily diffuse into the pores of PCU-HPC materials, their antibacterial activity being influenced by the content of ZnONPs. The antibacterial property of the membranes is attributed to the ZnONPs.³⁹

CONCLUSION

This study was performed on a series of PCU-HPC membranes with progressive amounts of ZnONPs. Young's modulus and tensile strength of the samples improved significantly to the detriment of elongation. In addition, hardness also increased with the increment of the amount of ZnONPs. Tensile toughness increased when a low amount of ZnONPs was incorporated in the sample. The hydrophobicity of these PCU-HPC membranes increased with a rise in the percentage of ZnONPs. Antibacterial activity was evaluated by determining the degree of turbidity, measuring the OD of the analyzed solutions. The antibacterial activity of these membranes was greater as the ZnONPs content was higher. The results suggest that the PCU-HPC membranes with ZnONPs can be used as antibacterial materials and the introduction of HPC into PCU with carboxylic sequence in the main chain extends their potential applications.

ACKNOWLEDGEMENTS: The authors express sincere thanks to Dr. Nita Tudorachi ("P. Poni" Institute of Macromolecular Chemistry, Iasi, Romania) for TG-DTG measurements.

REFERENCES

- O. Bayer, *Modern Plastics*, **24**, 149 (1947).
- J. Saunders and K. Frisch, "Polyurethanes: Chemistry and Technology", Parts I and II, Interscience Publishers, NY, 1967.

- M. D. Lelah and S. L. Cooper, "Polyurethanes in Medicine", CRC, Boca Raton, FL, 1986.
- G. Oertel, "Polyurethane Handbook", 2nd ed., Hanser Publishers, Munich, 1994.
- D. Klempner and K. Frisch, "Advances in Urethane Science and Technology", Rapra Publisher, UK, 2001.
- S. Vessot, J. Andrieu, P. Laurent, J. Galy and J. F. Gerard, *J. Coat. Technol.*, **70**, 67 (1998).
- S. Vlad, *Mater. Plast.*, **42**, 293 (2005).
- S. R. Yang, O. J. Kwon, D. H. Kim and J. S. Park, *Fiber. Polym.*, **8**, 257 (2007).
- D. Zvekic, V. V. Srdic, M. A. Karaman and M. N. Matavulj, *Process. Appl. Ceram.*, **5**, 41 (2011).
- S. Vlad and S. Oprea, *J. Optoelectron. Adv. M.*, **9**, 994 (2007).
- M. Bock, "Polyurethanes for Coatings", Curt R. Vincentz Verlag, Hannover, 2001.
- C. Guo, Z. Zheng, Q. Zhu and X. Wang, *Polym. Plast. Technol.*, **46**, 1161 (2007).
- P. Devos, Y. Baziard, B. Rives and P. Michelin, *J. Appl. Polym. Sci.*, **81**, 1848 (2001).
- S. Vlad, C. Ciobanu, D. Macocinschi, D. Filip and I. Spiridon, *J. Optoelectron. Adv. M.*, **11**, 1160 (2009).
- T. W. Cho and S. W. Kim, *J. Appl. Polym. Sci.*, **121**, 1622 (2011).
- P. Vermette, H. J. Griesser, G. Laroche and R. Guidoin, "Biomedical Applications of Polyurethanes", Eureka.com, 2001.
- S. Vlad, M. Butnaru, D. Filip, D. Macocinschi, A. Nistor *et al.*, *Dig. J. Nanomater. Bios.*, **5**, 1089 (2010).
- G. Saint-Pierre, M. Herrero Gomez, S. Martinez Creispera, A. Saiani, C. Merry *et al.*, WIPO Patent: WO 2014/044321 A1.
- M. Mandru, S. Vlad, C. Ciobanu, L. Lebrun and M. Popa, *Cellulose Chem. Technol.*, **47**, 5 (2013).
- D. Macocinschi, D. Filip, S. Vlad, M. Cristea, V. Musteata *et al.*, *J. Biomed. Appl.*, **27**, 119-129 (2012).
- J. J. Elsner, Y. Mezape, K. Hakshur, M. Shemesh, E. Linder-Ganz *et al.*, *Acta Biomater.*, **6**, 4698 (2010).

- ²² A. Eceiza, M. Larranaga, K. de la Caba, G. Kortaberria, C. Marieta *et al.*, *J. Appl. Polym. Sci.*, **108**, 3092 (2008).
- ²³ M. Spirkova, J. Pavlicevic, A. Strachota, R. Poreba, O. Bera *et al.*, *Eur. Polym. J.*, **47**, 959 (2011).
- ²⁴ S. Vlad, C. Tanase, D. Macocinschi, C. Ciobanu, T. Balaes *et al.*, *Dig. J. Nanomater. Bios.*, **7**, 51 (2012).
- ²⁵ S. Vlad, C. Ciobanu, R. V. Gradinaru, L. M. Gradinaru and A. Nistor, *Dig. J. Nanomater. Bios.*, **6**, 921 (2011).
- ²⁶ A. Yadav, V. Prasad, A. A. Kathe, S. Raj, D. Yadav *et al.*, *Bull. Mater. Sci.*, **29**, 641 (2006).
- ²⁷ O. Faruk, A. K. Bledzki, H.-P. Fink and M. Sain, *Prog. Polym. Sci.*, **37**, 1552 (2012).
- ²⁸ G. Stiubianu, M. Cazacu, A. Nicolescu, V. Hamciuc and S. Vlad, *J. Polym. Res.*, **17**, 837 (2010).
- ²⁹ M. Butnaru, D. Macocinschi, C. D. Dimitriu, S. Vlad, D. Filip *et al.*, *Optoelectron. Adv. Mat.*, **5**, 172 (2011).
- ³⁰ S. Vlad, D. Filip, D. Macocinschi, I. Spiridon, A. Nistor *et al.*, *Optoelectron. Adv. Mat.*, **4**, 407 (2010).
- ³¹ D. Macocinschi, D. Filip, S. Vlad, M. Butnaru and L. Knieling, *Int. J. Biol. Macromol.*, **52**, 32 (2013).
- ³² M. Butnaru, O. Bredetean, D. Macocinschi, C. D. Dimitriu, L. Knieling *et al.*, in "Polyurethane", edited by F. Zafar and E. Sharmin, InTech, 2012, Ch. 10.
- ³³ S. Maiti, D. Krishnan, G. Barman, S. K. Ghosh and J. K. Laha, *J. Anal. Sci. Technol.*, **5**, 40 (2014).
- ³⁴ N. Dragoe, D. Fatu and E. Segal, *J. Therm. Anal. Cal.*, **55**, 977 (1999).
- ³⁵ J. Crank, "The Mathematics of Diffusion", 2nd ed., Clarendon Press, Oxford, 1975.
- ³⁶ C. M. Balik, *Macromolecules*, **29**, 3025 (1996).
- ³⁷ R. N. Darie, S. Vlad, N. Anghel, F. Doroftei, T. Tamminen, I. Spiridon, *Polym. Adv. Technol.*, **26**, 941 (2015).
- ³⁸ T. Thomson, "Polyurethanes as Specialty Chemicals: Principles and Applications", CRC Press LLC, 2000.
- ³⁹ J. Sawai, S. Shoji, H. Igarashi, A. Hashimoto, T. Kokugan *et al.*, *J. Ferment. Bioeng.*, **86**, 521 (1998).